IOPscience iopscience.iop.org

Home Search Collections Journals About Contact us My IOPscience

Performance Enhancement of *a*-Plane Light-Emitting Diodes Using InGaN/GaN Superlattices

This content has been downloaded from IOPscience. Please scroll down to see the full text.

2009 Jpn. J. Appl. Phys. 48 04C136

(http://iopscience.iop.org/1347-4065/48/4S/04C136)

View the table of contents for this issue, or go to the journal homepage for more

Download details:

IP Address: 140.113.38.11
This content was downloaded on 25/04/2014 at 10:40

Please note that terms and conditions apply.

Performance Enhancement of *a*-Plane Light-Emitting Diodes Using InGaN/GaN Superlattices

Shih-Chun Ling[1], Te-Chung Wang[1,2], Jun-Rong Chen[1], Po-Chun Liu[2], Tsung-Shine Ko[1], Tien-Chang Lu[1], Hao-Chung Kuo[1], Shing-Chung Wang[1], and Jenq-Dar Tsay[2]

[1] *Department of Photonics and Institute of Electro-Optical Engineering, National Chiao Tung University, 1001 University Road, Hsinchu, Taiwan 300, R.O.C.*
[2] *Electronics and Optoelectronics Research Laboratories, Industrial Technology Research Institute, 195 Chung Hsing Rd., Sec. 4 Chu Tung, Hsinchu, Taiwan 310, R.O.C.*

Received September 22, 2008; revised November 26, 2008; accepted December 11, 2008; published online April 20, 2009

We have fabricated *a*-plane light-emitting diodes (LEDs) with inserted InGaN/GaN superlattices. The structural characteristics and device performance of *a*-plane light-emitting diodes with/without superlattices were also identified. Transmission electron microscope (TEM) images revealed that the threading dislocation (TD) density for the sample using superlattices was reduced from 3×10^{10} cm^{-2} down to $\sim 9 \times 10^{9}$ cm^{-2}. The electroluminescence (EL) intensity of the sample with InGaN/GaN superlattices was enhanced by a factor of 3.42 times to that of the conventional sample without InGaN/GaN superlattices. Furthermore, we observed that the polarization degree of *a*-plane LEDs with superlattices (56.3%) was much higher than that without superlattices (27.4%). A series of experiments demonstrated that the feasibility of using InGaN/GaN superlattices for the TD reduction and the improvement of luminescence performance in *a*-plane III–nitride devices. © 2009 The Japan Society of Applied Physics

DOI: 10.1143/JJAP.48.04C136

1. Introduction

Recently, nitride-based light-emitting diodes (LEDs) have been attracting great attention owing to the potential application in solid-state lighting. However, the conventional *c*-plane nitride-based quantum wells exhibit the quantum-confined Stark effect[1,2] as a result of the existence of spontaneous and piezoelectric polarization fields that are parallel to [0001] *c*-direction. This effect results in spatial separation of the electron and hole wave functions in the quantum wells, which restricts the carrier recombination efficiency, reduces oscillator strength, and induces red-shifted emission.[3] To avoid such polarization effects, growth along [11$\bar{2}$0]-oriented direction has been explored for planar *a*-plane GaN prepared on *r*-plane sapphire[4] and *a*-plane SiC[5] by metalorganic vapor phase deposition (MOCVD). Since these GaN surfaces contain an equal number of Ga and N atoms in each monolayer, a free electric field and nonpolar characteristic are obtained. The recent studies of *a*-plane AlGaN/GaN[6,7] and InGaN/GaN[8,9] multi-quantum wells (MQWs) demonstrate that it is possible to eliminate such polarization fields along nonpolar orientation. In addition, nonpolar LEDs have been shown to exhibit optically polarized spontaneous emission, which is explained to be a result of the crystal field oriented along the *c*-axis of wurtzite GaN and its effect on the valence band splitting induced by large compressive strain within the wells.[10,11] Therefore, the use of these polarized light emitters in liquid crystal display units is a great chance to save energy owing to the elimination of a sheet polarizer.[12] However, the difficult issue is that there is no suitable substrate for heteroepitaxial planar *a*-plane GaN growth.

In general, there is a threading dislocation (TD) density of $\sim 3 \times 10^{10}$ cm^{-2} and a basal stacking fault density of $\sim 3.5 \times 10^{5}$ cm^{-1} in *a*-plane GaN grown on *r*-plane sapphire structure because of the large lattice mismatch.[13] The TDs in GaN act as nonradiative recombination centers to restrict internal quantum efficiency. Therefore, the reduction of threading dislocation density is essential to improve device performance. Lateral epitaxial overgrowth (LEO) techniques have been employed in the past to achieve defect reduction in nonpolar GaN.[14–18] However, all of these LEO techniques involve *ex-situ* processing steps and it is difficult to control the uniformity of the regrowth thickness exceeding 20 μm required for coalescence. Another possible method for reducing threading dislocation density is to insert strain-layer superlattices into the epitaxial layer. The strain which is due to different lattice constants in the superlattices, can deflect the threading dislocation into the interfacial plane and has been theoretically analyzed by Matthews and Blakeslee.[19,20] The dislocation line that runs parallel to the growth direction is bowed as a result of the coherent strain present in the superlattices. Subsequently, the dislocations move laterally and are eliminated with other dislocations of the opposite Burgers vector, or combine with a dislocation of a different Burgers vector to form a third one, or even run to the edge of the wafer. Ultimately, dislocation density reduction is achieved by the insertion of superlattices. In this study, we utilize the strain mechanism to realize defect reduction in *a*-plane LEDs and demonstrate the performance improvement of *a*-plane LEDs using InGaN/GaN superlattices. Unlike these traditional LEO techniques, this dislocation reduction method is highly advantageous due to the simplicity and low cost.

2. Experiments

First, a low temperature GaN nucleation layer was grown by low pressure metal-organic chemical vapor deposition (MOCVD) on *r*-plane sapphire substrates, followed by the growth of 0.5-μm-thick high temperature GaN. Then, a superlattices comprising 20 pairs of 5-nm-thick $In_{0.2}Ga_{0.8}N$ and 5-nm-thick GaN were inserted and subsequently a 1.5-μm-thick Si-doped n-GaN with an electron concentration of 3×10^{18} cm^{-3} was grown. Afterward, a MQWs consisting 10 pairs of 6-nm-thick wells and 15-nm-thick barriers was grown at a temperature of 827 °C and capped by a 0.15-μm-thick p-GaN layer with a hole concentration of 6×10^{17} cm^{-3}. The structure of the *a*-plane LED is shown in Fig. 1. The as-grown samples were investigated by transmission

 © 2009 The Japan Society of Applied Physics

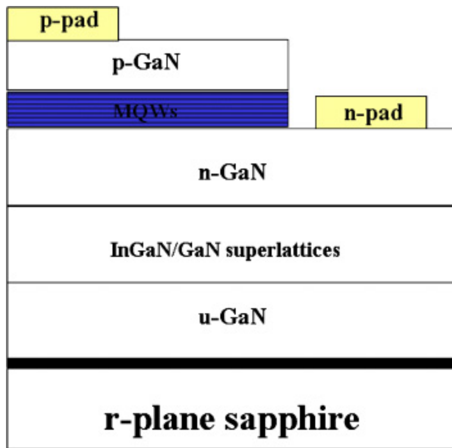

Fig. 1. (Color online) Structure of *a*-plane LED with the insertion of InGaN/GaN superlattices.

electron microscopy (TEM) to compare the microstructures of *a*-plane LEDs grown with and without InGaN/GaN superlattices. Temperature-dependent micro-photoluminescence (μ-PL) measurements were carried out using the 405 nm line of a CW InGaN laser diode with a spot size of 10 μm over the temperature range 90–300 K. Then, $300 \times 300\,\mu m^2$ diode mesas were defined by chlorine-based reactive ion etching. Ti/Au (100/200 nm) and Ti/Al/Pt/Au (30/180/40/150 nm) were used as p- and n-GaN contacts, respectively. The electroluminescence (EL) and polarization characteristics of the diodes were measured by on-wafer probing of the devices.

3. Results and Discussion

To demonstrate the dislocation reduction of the *a*-plane LED with the insertion of InGaN/GaN superlattices, TEM was performed to compare the microstructures of *a*-plane LEDs with and without superlattices. The typical bright-field cross-sectional TEM image of the sample with superlattices near $[1\bar{1}00]_{GaN}$ zone axis is shown in Fig. 2(a). The inset of Fig. 2(a) presents the corresponding electron diffraction pattern. From the TEM image, significant blocking of TDs was observed at the n-GaN/superlattices interface. Thus it was apparent that the insertion of InGaN/GaN superlattices can reduce the dislocation density effectively. The estimated threading dislocation density was reduced from 3×10^{10} cm^{-2} down to $\sim 9 \times 10^{9}\,cm^{-2}$. Figures 2(b) and 2(c) show the MQWs grown on the template without and with superlattices, respectively. As shown in Fig. 2(b), the boundaries between InGaN wells and GaN barriers were severely interfered by lots of TDs parallel to the $(11\bar{2}0)$ growth direction that would give rise to the poor carrier confinement and low internal quantum efficiency. In contrast, as shown in Fig. 2(c), the MQWs revealed a clearer boundary between InGaN wells and GaN barriers than that of Fig. 2(b). In order to confirm the quality improvement of *a*-plane MQWs using InGaN/GaN superlattices, Arrhenius plots of the normalized integrated PL intensity for the *a*-plane LED without and with InGaN/GaN superlattices over the temperature range 90–300 K were measured. The 405 nm line of InGaN laser diode was used as a PL pumping source to avoid the absorption in GaN and prevent the excess photo-generated carriers from being injected into MQWs. Therefore, the effective excitation conditions are the same for the MQWs grown on the templates with and without superlattices. Sample 1 and Sample 2 are the *a*-plane LED without and with InGaN/GaN superlattices, respectively. Figures 3(a) and 3(b) show the normalized integrated PL as a function of $1000/T$ for Sample 1 and Sample 2, respectively, wherein the thermal activation energies of 86.15 and 118.7 meV were estimated from the Arrhenius plots. Furthermore, the integrated PL intensity ratio obtained at 90 and 300 K $[I_{PL}(300\,K)/I_{PL}(90\,K)]$ for Sample 2, which is approximately 16%, is larger than that of Sample 1 (nearly 10.3%). In general, the temperature-induced quenching of luminescence involves

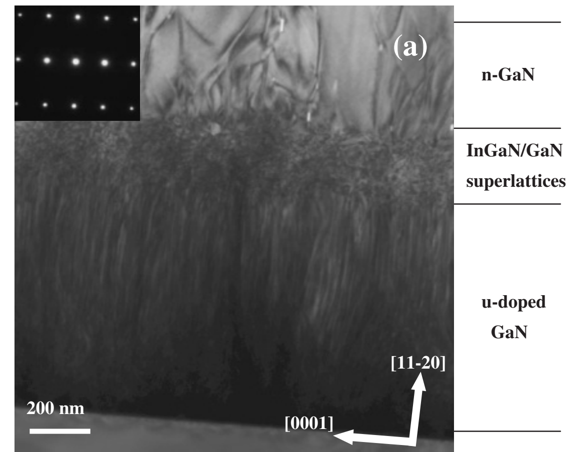

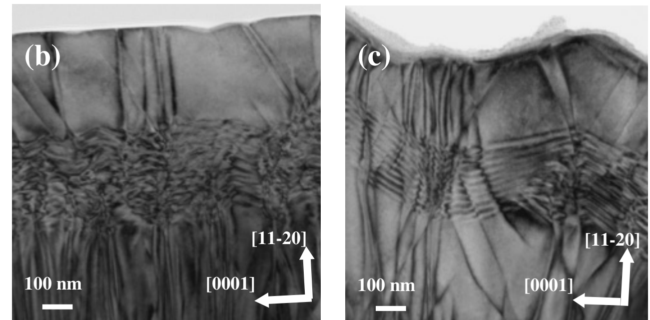

Fig. 2. (a) Cross-sectional TEM image of *a*-plane LED with superlattices. Inset shows the corresponding electron diffraction pattern. Morphologies of MQWs grown on the templates (b) without and (c) with superlattices are also shown.

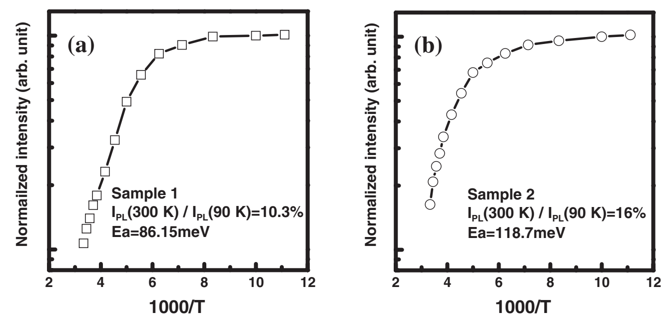

Fig. 3. Arrhenius plots of the normalized integrated PL intensity over the temperature range 90–300 K for (a) Sample 1 and (b) Sample 2.

© 2009 The Japan Society of Applied Physics

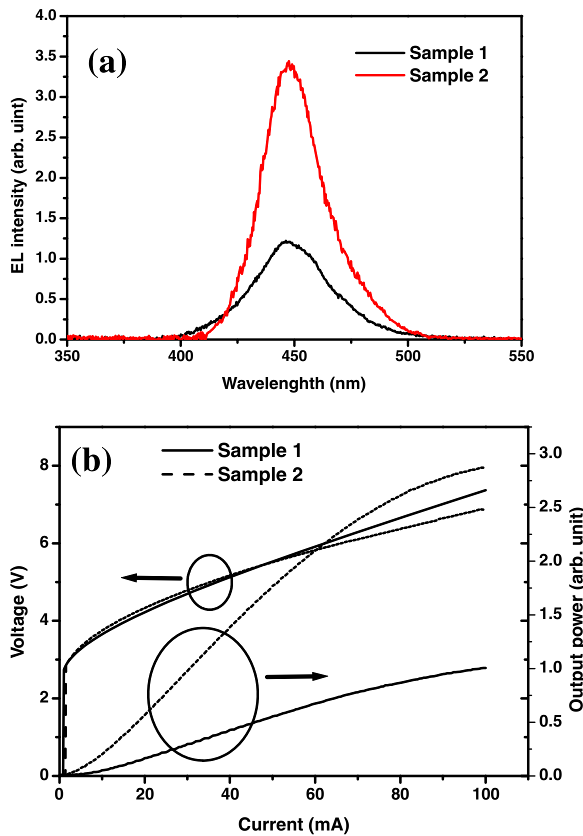

Fig. 4. (Color online) (a) Room-temperature EL spectra and (b) *L–I–V* curves for Sample 1 and Sample 2.

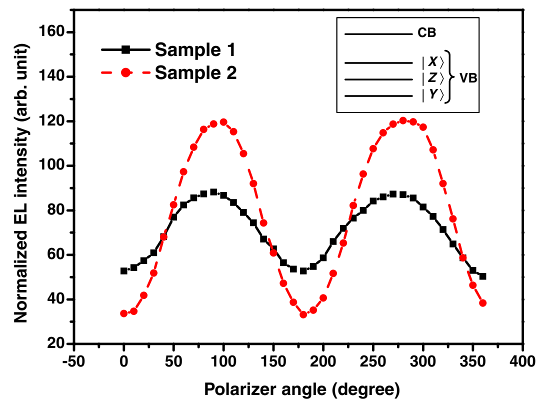

Fig. 5. (Color online) EL intensity of Sample 1 and Sample 2 at different polarization angles at 20 mA injection current.

the thermal emission of charge carriers out from confined quantum-well states into barrier states,[21,22] the thermal dissociation of excitons into free electron–hole pairs,[23] and the thermal activation of excitons to non-radiative defect states.[24] Therefore, the thermal activation energy is a quantity to measure the exciton binding energy or the energy difference between the energy of the quantum-well confined state and the barrier continuum state or defect state. As a result, the carrier confinement of *a*-plane MQWs was indeed enhanced in terms of activity energy estimation by introducing InGaN/GaN superlattices.

Room-temperature EL spectra under 20 mA injection current is shown in Fig. 4(a). The same emission peaks were located at 449 nm for both samples. The EL full width at half maximum (FWHM) of Sample 2 was measured as 28.7 nm, which was narrower than that of Sample 1 (FWHM = 35.8 nm). The *L–I–V* curves were measured to further demonstrate the performance enhancement of *a*-plane LEDs with InGaN/GaN superlattices as shown in Fig. 4(b). These two *I–V* curves exhibited similar shapes, indicating that the absence of the degradation of electrical characteristics with the insertion of superlattices. The forward voltages of Sample 1 and Sample 2 were both 4.25 V at 20 mA operating current. The series resistances of Sample 1 and Sample 2 were estimated to be $\sim$24 Ω. The output power of Sample 2 had a 3.42- and 2.86-fold increase compared with those of Sample 1 at 20 and 100 mA injection current, respectively. Such an apparent enhancement was attributed to the dislocation reduction and the improvement of the MQW quality upon inserting InGaN/GaN superlattices.

The *a*-plane (In,Ga)N films suffer from anisotropic in-plane compressive strain in the x–y plane (x is oriented along $\langle 1\bar{1}00\rangle$, y is oriented along $\langle 11\bar{2}0\rangle$, and z is oriented along $\langle 0001\rangle$) of the wurtzite crystal and the original $|X \pm iY\rangle$-like valence-band states of unstrained wurtzite crystal are split into $|X\rangle$- and $|Y\rangle$-like states. The energy of the $|X\rangle$-like state is raised by the strain, while that of the $|Y\rangle$-like state is pushed down to below that of the $|Z\rangle$-like state (see the inset of Fig. 5). Therefore, electronic transitions occur predominantly from the bottom of the conduction band to the topmost $|X\rangle$-like state and the resulting light emission will have a strong x-polarized ($\mathbf{E} \perp c$) characteristic.[10,11] In order to analyze the linear polarization of the EL of our devices, we rotated a polarizer between the polarization angle of 0° (parallel to the c-axis) and 360°. The polarization ratio is defined as $\rho = (I_{\max} - I_{\min})/(I_{\max} + I_{\min})$, where $I_{\max}$ is the intensity of light with polarization perpendicular to the c-axis and $I_{\min}$ is the intensity of light with polarization parallel to the c-axis. Figure 5 shows the EL intensities of Sample 1 and Sample 2 at different polarization angles at room temperature. The degree of polarization of Sample 2, which was estimated to be approximately 56.3%, was larger than that of Sample 1 (nearly 27.4%). There are two possible reasons that account for this phenomenon. First, the TDs in GaN act as nonradiative recombination centers and could restrict the carrier transitions from the bottom of the conduction band to the topmost $|X\rangle$-like state. Since the superlattices can reduce the dislocation density, the severe interruption of selective carrier transition was reduced. The other reason is that the superlattices may amplify the anisotropic in-plane compressive strain experienced by the MQWs and consequently give rise to a higher transition energy difference between the $|X\rangle$-like state and $|Z\rangle$-like state. As a result, the polarized characteristic of *a*-plane LEDs with superlattices was enhanced.

4. Conclusions

We have demonstrated that the performance enhancement of *a*-plane LEDs was achieved by the insertion of InGaN/GaN superlattices. The threading dislocation density was reduced from 3×10^{10} to $\sim 9 \times 10^{9}$ cm^{-2}. From the Arrhenius plots, the thermal activation energy of the sample with InGaN/GaN superlattices which was estimated to be 105.3 meV, was larger than that of the sample without InGaN/GaN

© 2009 The Japan Society of Applied Physics

superlattices (83.7 meV). Afterward, the EL intensity of the sample with InGaN/GaN superlattices exhibited improvement by a factor of 3 in comparison with that of the conventional sample without InGaN/GaN superlattices, which could be attributed to the TD reduction and the improvement of LED quality. Furthermore, we observed that the polarization degree of *a*-plane LEDs with superlattices (56.3%) was much higher than that of *a*-plane light emitting diodes without superlattices (27.4%).

Acknowledgements

This work was supported by the Ministry of Economic Affairs of the Republic of China (MOEA). The number of the project was 7301XS1G20 for the nonpolar GaN epitaxy and MOVPE part. Also, the authors would like to thank Professor Chia-Feng Lin at National Chung Hsing University (NCHU) for assistance in the PL measurement.

1) T. Takeuchi, S. Sota, M. Katsuragawa, M. Komori, H. Takeuchi, H. Amano, and I. Akasaki: Jpn. J. Appl. Phys. **36** (1997) L382.
2) D. A. B. Miller, D. C. Chemla, T. C. Damen, A. C. Grossard, W. Wiegmann, T. H. Wood, and C. A. Burrus: Phys. Rev. B **32** (1985) 1043.
3) J. S. Im, H. Kollmer, J. Off, A. Sohmer, F. Scholz, and A. Hangleiter: Phys. Rev. B **57** (1998) 9435.
4) M. D. Craven, S. H. Lim, F. Wu, J. S. Speck, and S. P. DenBaars: Appl. Phys. Lett. **81** (2002) 469.
5) M. D. Craven, A. Chakraborty, B. Imer, F. Wu, S. Keller, U. K. Mishra, J. S. Speck, and S. P. DenBaars: Phys. Status Solidi C **0** (2003) 2132.
6) G. A. Garrett, H. Shen, M. Wraback, B. Imer, B. Haskell, J. S. Speck, S. Keller, S. Nakamura, and S. P. DenBaars: Phys. Status Solidi A **202** (2005) 846.
7) H. M. Ng: Appl. Phys. Lett. **80** (2002) 4369.
8) A. Chakraborty, B. A. Haskell, S. Keller, J. S. Speck, S. P. DenBaars, S. Nakamura, and U. K. Mishra: Appl. Phys. Lett. **85** (2004) 5143.
9) A. Chakraborty, S. Keller, C. Meier, B. A. Haskell, S. Keller, P. Waltereit, S. P. DenBaars, S. Nakamura, J. S. Speck, and U. K. Mishra: Appl. Phys. Lett. **86** (2005) 031901.
10) B. Rau, P. Waltereit, O. Brandt, M. Ramsteiner, K. H. Ploog, J. Puls, and F. Henneberger: Appl. Phys. Lett. **77** (2000) 3343.
11) Y. J. Sun, O. Brandt, M. Ramsteiner, H. T. Grahn, and K. H. Ploog: Appl. Phys. Lett. **82** (2003) 3850.
12) H. Masui, H. Yamada, K. Iso, S. Nakamura, and S. P. DenBaars: Appl. Phys. Lett. **92** (2008) 091105.
13) M. D. Craven, S. H. Lim, F. Wu, J. S. Speck, and S. P. DenBaars: Appl. Phys. Lett. **81** (2002) 469.
14) M. D. Craven, S. H. Lim, F. Wu, J. S. Speck, and S. P. DenBaars: Appl. Phys. Lett. **81** (2002) 1201.
15) C. Chen, J. Zhang, J. Yang, V. Adivarahan, S. Rai, S. Wu, H. Wang, W. Sun, M. Su, Z. Gong, E. Kuokstis, M. Gaevski, and M. A. Khan: Jpn. J. Appl. Phys. **42** (2003) L818.
16) B. Imer, F. Wu, S. P. DenBaars, and J. S. Speck: Appl. Phys. Lett. **88** (2006) 061908.
17) T. C. Wang, T. C. Lu, T. S. Ko, H. C. Kuo, M. Yu, and S. C. Wang: Appl. Phys. Lett. **89** (2006) 251109.
18) B. A. Haskell, F. Wu, M. D. Craven, S. Matsuda, P. T. Fini, T. Fujii, K. Fujito, S. P. DenBaars, J. S. Speck, and S. Nakamura: Appl. Phys. Lett. **83** (2003) 644.
19) J. W. Matthews and A. E. Blakeslee: J. Cryst. Growth **27** (1974) 118.
20) J. W. Matthews and A. E. Blakeslee: J. Cryst. Growth **32** (1976) 265.
21) S. Weber, W. Limmer, K. Thonke, R. Sauer, K. Panzlaff, G. Bacher, H. P. Meier, and P. Roentgen: Phys. Rev. B **52** (1995) 14739.
22) Y. T. Shih, Y. L. Tsai, C. T. Yuan, C. Y. Chen, C. S. Yang, and W. C. Chou: J. Appl. Phys. **96** (2004) 7267.
23) I. Y. Gerlovin, Y. K. Dolgikh, V. V. Ovsyankin, Y. P. Efimov, I. V. Ignat'ev, and E. E. Novitskaya: Phys. Solid State **40** (1998) 1041.
24) Y. h. Wu, K. Arai, and T. Yao: Phys. Rev. B **53** (1996) 10485.

© 2009 The Japan Society of Applied Physics